Legionella pneumophila Is Internalized by a Macropinocytotic Uptake Pathway Controlled by the Dot/Icm System and the Mouse *Lgn1* Locus✪

Masahisa Watarai,[1,2] Isabelle Derre,[2] James Kirby,[2] Joseph D. Growney,[3] William F. Dietrich,[1,3] and Ralph R. Isberg[1,2]

[1]*Howard Hughes Medical Institute, and the* [2]*Department of Molecular Biology and Microbiology, Tufts University School of Medicine, Boston, MA 02111*
[3]*Department of Genetics, Harvard Medical School, Boston, MA 02115*

Abstract

The products of the *Legionella pneumophila dot/icm* genes enable the bacterium to replicate within a macrophage vacuole. This study demonstrates that the Dot/Icm machinery promotes macropinocytotic uptake of *L. pneumophila* into mouse macrophages. In mouse strains harboring a permissive *Lgn1* allele, *L. pneumophila* promoted formation of vacuoles that were morphologically similar to macropinosomes and dependent on the presence of an intact Dot/Icm system. Macropinosome formation appeared to occur during, rather than after, the closure of the plasma membrane about the bacterium, since a fluid-phase marker preloaded into the macrophage endocytic path failed to label the bacterium-laden macropinosome. The resulting macropinosomes were rich in GM1 gangliosides and glycosylphosphatidylinositol-linked proteins. The *Lgn1* allele restrictive for *L. pneumophila* intracellular replication prevented *dot/icm*-dependent macropinocytosis, with the result that phagosomes bearing the microorganism were targeted into the endocytic network. Analysis of macrophages from recombinant inbred mouse strains support the model that macropinocytotic uptake is controlled by the *Lgn1* locus. These results indicate that the products of the *dot/icm* genes and *Lgn1* are involved in controlling an internalization route initiated at the time of bacterial contact with the plasma membrane.

Key words: *Legionella pneumophila* • macropinocytosis • Lgn1 • vacuole • *dot/icm*

Introduction

A central aspect of Legionnaires' disease is the growth of *Legionella pneumophila* within alveolar macrophages after inhalation of aerosolized fresh water supplies containing *L. pneumophila*. In culture, growth of *L. pneumophila* can be observed within monocytes and macrophages (1), as well as within amoebae, the presumed natural reservoir (2–4). Intracellular replication has been demonstrated to be an essential virulence determinant in animal models (5).

A number of morphological studies have detailed the intracellular lifecycle of *L. pneumophila* within phagocytic cells. The most striking aspect of intracellular growth is that, shortly after uptake, the organism is found in a vacuole devoid of most endocytic markers which appears to bypass fusion with the host cell lysosomal network (6, 7). This specialized compartment eventually associates with small vesicles, mitochondria, and rough endoplasmic reticulum, forming a niche in which the organism replicates to large numbers (8, 9). The vacuole bears some morphological similarity to autophagous compartments (9). At time periods >6 h after uptake, the resistance to fusion with the endocytic network appears to break down in >50% of the replication vacuoles. At these later time points, acidification and fusion events may be required for efficient intracellular growth (10).

Formation of the replication vacuole in mammalian macrophages requires the products of a majority of the 25 *dot/icm* genes (11). At least 16 of the predicted protein products of these genes show high sequence similarity to bacterial proteins involved in conjugative DNA transfer (12). Furthermore, the Dot/Icm system has retained the ability to promote DNA transfer to other bacterial cells (11,

---

13). The implication from this conservation of sequence and function is that the Dot/Icm system is a protein complex that transfers effector macromolecules from the bacterium to the target mammalian cell.

Several studies indicate that Dot/Icm acts at extremely early times after interaction of the bacterium with the target host cell to direct formation of the vacuole (14–16). In contrast to wild-type strains, mutations in dot/icm genes result in accumulation of the late endosomal marker lysosomal-associated membrane protein (LAMP)-1 about the phagosome as early as 5 min after contact with the bacterium (14, 15). The primary requirement for Dot/Icm activity during internalization of the microorganism demonstrated by these studies indicates that this system may be involved in promoting uptake of the bacterium.

Initial work on the mechanism of uptake by macrophages indicates that some serotypes of L. pneumophila are internalized by a process called coiling phagocytosis, in which a unilateral pseudopod rolls into itself rather than fuses with its stem (7). Not all serotypes are internalized via this mechanism (17), and no correlation has been demonstrated between the dot/icm genotype of the organism and the ability to promote coiling (7). The phagocytic receptor bound by the organism on the surface of the target host cell appears to play little role in determining the ultimate fate of the organism, since opsonization with antibody does not prevent intracellular growth (1, 18, 19). Furthermore, L. pneumophila grows efficiently in amoebae, although the bacteria are internalized into these cells via a receptor not found on macrophages (20). Therefore, if L. pneumophila induces a specific uptake pathway after binding host cells, it must bypass signals sent from any receptor bound by the bacterium that may potentially target the phagosome into a degradative pathway.

Genetic evidence points to at least one locus encoded by the host that controls the ability of L. pneumophila to undergo efficient intracellular replication (21, 22). With the exception of the A/J mouse, most inbred mouse strains are highly resistant to L. pneumophila disease, and macrophages isolated from these strains yield little or no growth of the microorganism (23). Crosses between the permissive A/J and the highly restrictive C57BL/6J strains have mapped the difference between these two strains to a single locus called Lgn1, located on chromosome 13 (21, 22). Lgn1 is within a series of highly polymorphic repeats of the mouse neuronal apoptosis inhibitory protein gene (Naip), in a region that varies greatly between different inbred mouse strains (24, 25). The only two expressed genes in the region defined by Lgn1 (Naip2 and Naip5) are uncharacterized and have no defined function in the cell, in spite of their similarity to apoptotic inhibitory proteins encoded by baculoviruses (26). No attempt has been made to determine the point at which the restrictive Lgn1 allele blocks L. pneumophila replication.

In this report, we describe a novel phagocytic pathway promoted by the dot/icm system of L. pneumophila. The pathway appears similar to macropinocytosis, is associated with recruitment of a subset of membrane proteins, and is blocked in recombinant inbred (RI)* mouse strains that are restrictive for L. pneumophila growth.

Materials and Methods

Reagents

TRITC-tetramethylrhodamine isothiocyanate dextran of molecular weight 155,000 (Rh-Dx155) was obtained from Sigma-Aldrich. Anti–L. pneumophila polyclonal rabbit serum was described previously (27) as was rabbit anti-Rab7 (14, 28). Goat anti–rabbit IgG cascade blue, goat anti–rat IgG-RITC, and rhodamine-phalloidin were obtained from Molecular Probes. Anti–LAMP-1 rat monoclonal antibody ID4B was obtained from Developmental Studies Hybridoma Bank of the Department of Pharmacology and Molecular Sciences, Johns Hopkins University School of Medicine, Baltimore, MD, and the Department of Biology, University of Iowa, Iowa City, Iowa. Biotinylated cholera toxin B (biotin-CTB) subunit was obtained from List Biological Laboratories and Alexa594-aerolysin was obtained from Protox Biotech.

Bacterial Strains, Mice, and Media

All L. pneumophila derivatives are from LP01 (hsdR rpsL), a virulent L. pneumophila Philadelphia-1, serogroup 1 strain that grows intracellularly (29). LP02 (hsdR rpsL thyA) and LP03 (LP02 dotA) have been described previously (29). The derivation and characterization of the plasmid pAM239 encoding green fluorescent protein (GFP) (30), as well as MW028 (dotH), HL056 (dotI), and MW037 (dotO) have been described previously (27, 30). Lp02- or Lp03-pH6 antigen containing strains have pAY68 (a plasmid expressing the pH6 antigen pilus of Yersinia pseudotuberculosis) (31). L. pneumophila strains were maintained as described previously (9, 32, 33). 1 mM isopropylthio-β-D-galactoside was used for induction of GFP and 5 μg/ml chloramphenicol was used for maintenance of pAM239. Opsonization of bacteria with rabbit anti–L. pneumophila serum was described previously (34). A×B and B×A mouse strains are RI strains that are crosses between A/J and C57BL/6J. All mice were purchased from The Jackson Laboratory.

Cell Culture

Bone marrow–derived macrophages from female A/J and C57BL/6J mice were prepared as described previously (9). After culturing in L-cell–conditioned medium, the macrophages were replated for use by lifting cells in PBS on ice for 5–10 min, harvesting cells by centrifugation, and resuspending cells in RPMI 1640 containing 10% heat inactivated FBS and glutamine. The macrophages were seeded (2–3 $\times 10^5$ cells per well) in a 24-well tissue culture plate for all assays.

Assay for Intracellular Growth

L. pneumophila strains were grown in ACES-buffered yeast extract containing 100 μg/ml thymidine (29) to $A_{600} = 3.2$, diluted in RPMI 1640, and introduced onto monolayers of 3 $\times$ 10^5 bone marrow macrophages in 24-well culture dishes at the

indicated multiplicity of infection (MOI) by centrifugation for 5 min. The cultures were incubated for 10 min at 37°C, 5% CO_2 to allow for maximal macropinosome formation, washed, and incubated with medium containing 50 μg/ml gentamicin for 30 min. The monolayers were then washed three times to remove the antibiotic, and bacterial titers were determined in half the monolayers (bacterial counts at t = 0 h). Fresh medium was added to the other monolayers and bacterial growth was quantitated 24 h later by determining total viable counts present in the culture well. t_{24}/t_0 = bacterial counts at 24 h per bacterial counts determined after 30 min gentamicin treatment.

Time Lapse Video Microscopy

Bone marrow–derived macrophages (10^6 cells) were plated on 20-mm round coverslips and allowed to incubate overnight in RPMI 1640 containing 10% FCS at 37°C in 5% CO_2. A 20-mm rubber O ring was then coated with vacuum grease, placed on a microscope slide, and ~200 μl of fresh prewarmed RPMI 1640 medium containing 10^6 cells per milliliter bacteria was added to the O-ring chamber. A coverslip having a monolayer of macrophages was then placed on top of the grease-coated O ring. The chamber was then inverted and placed on a heated microscope stage set to 37°C for observation using a Nikon TE300 inverted phase microscope with a 100X Plan Neofluor lens fitted with phase contrast optics. The bacteria were allowed to passively pellet onto the macrophages, and images were captured over a 20-min period. If further observations were desired, new samples were prepared.

Detection of Intracellular Bacteria and Macropinosome Formation

L. pneumophila strains were grown to A_{600} = 3.2 in ACES-buffered yeast extract containing 100 μg/ml thymidine and used to infect mouse bone marrow–derived macrophages for various lengths of time at an indicated MOI. Bacteria in 250 μl of RPMI 1640 containing 1 mg/ml of Rh-Dx155 were deposited onto the macrophages by 150× *g* centrifugation for 5 min at room temperature, and were then incubated at 37°C for 0 (no incubation), 10, 20, and 30 min. Infected cells were fixed in periodate-lysine paraformaldehyde (PLP) containing 5% sucrose for 1 h at 37°C (35). To identify extracellular bacteria, samples were washed three times in PBS, fixed, and incubated with anti–*L. pneumophila* polyclonal rabbit serum diluted 1:10,000 in blocking buffer (2% goat serum in PBS) for 1 h at 37°C in the absence of permeabilization, as described previously (36). The preparations were then stained with a 1:500 dilution of goat anti–rabbit IgG cascade blue to label the extracellular bacteria. 100 macrophages were examined per coverslip to determine the total number of intracellular bacteria, macropinosome formation, and total number of bacteria within macropinosomes.

F-actin Staining

Bacteria were deposited onto the macrophages by 150× *g* centrifugation for 5 min at room temperature, or were allowed to bind passively if they were expressing pH 6.0 antigen pilus, and were then incubated at 37°C for the indicated times. Infected macrophages were fixed in PLP–sucrose for 1 h at 37°C, and stained for extracellular bacteria as described previously. Then, samples were permeabilized in 0.1% Triton X-100, washed three times with PBS, and incubated with rhodamine-phalloidin for 30 min at 37°C. After three washes with PBS, samples were mounted as above.

Colocalization of Proteins with Macropinosomes

To detect localization of GM1 gangliosides in macropinosomes, macrophage monolayers were incubated for 5 min with biotin-CTB, rinsed three times in RPMI 1640, and incubated with either LP02-GFP or LP03-GFP for the indicated time periods at 37°C (37). The cells were washed once, fixed in PLP–sucrose, and probed for extracellular bacteria, as above, before permeabilization in 0.05% saponin for 10 min at room temperature. After three washes with PBS and incubation in blocking buffer, the biotin-CTB was detected with RITC-streptavidin (1:500 in blocking buffer). To detect glycosylphosphatidylinositol (GPI) linkages, samples fixed as above were permeabilized in methanol at −20°C for 10 s and probed with Alexa594-aerolysin for 1 h at 37°C. Extracellular bacteria were detected as above. Analysis of LAMP-1 Rab7 and CD44 colocalization were as described previously (14, 36).

Assay for L. pneumophila-induced Cytotoxicity

3×10^5 bone marrow–derived macrophages were seeded on coverslips in 24-well culture dishes as above, and bacteria were introduced onto the monolayers at the indicated MOI, by centrifugation for 5 min. The cultures were incubated for 10 min at 37°C, 5% CO_2 to allow for maximal macropinosome formation, washed, and incubated 60 min further to allow cytotoxicity (34). The number of dead macrophages was determined microscopically by incubation in the presence of ethidium bromide (EtdBr) and acridine orange, counting number of EtdBr-permeable cells relative to total acridine orange-staining cells (34).

Genotype Determination of RI Mouse Strains

All STSs (sequence-tagged sites) were amplified as described previously (38). Primers for microsatellite markers were end labeled with [^{32}P]ATP, 6,000 Ci/mmol (NEN Life Science Products) and PCR products amplified as described previously (39). Amplification products were resolved on a 6% denaturing polyacrylamide gel (National Diagnostics) at 120 W for 3–4 h. Microsatellite markers D13Die3, D13Die6, D13Die7, D13Mit146, D13Die25, D13Die26, and D13Die36 have been described previously (24, 38, 40, 41).

Online Supplemental Material

Online are three movies that show typical interactions between *L. pneumophila* and bone marrow macrophages derived from A/J mice (video available at http://www.jem.org.cgi/content/full/194/8/1081/F1/DC1). Macrophages were incubated in sealed chambers using the described microscopy system (Materials and Methods), and images were captured approximately every 2.6 s using phase contrast microscopy with a 100×1.3 NA lens. The captured images are displayed as movies at 10 frames per second, so the movies are ~26× real time.

Video 1: Macropin (LP02). This shows the formation of a macropinosome about several bacteria being internalized simultaneously. The video begins with arrows pointing to several bacteria (LP02, Dot/Icm system intact) which are in the process of being trapped within a large ruffle forming about the surface of the macrophage. As the ruffle contracts around the bacteria, a compartment forms containing several bacteria that is significantly larger in volume than the bacteria. The compartment then rapidly decreases in size, to eventually form a vacuole that is tightly apposed to the group of bacteria. A series of fluid-containing compartment can be seen contacting the vacuole, but none of them fuse with the vacuole bearing the bacteria.

Video 2: Ruffle (LP02). This shows the induction of a large phase transparent puff in response to binding of a bacterium (LP02, Dot/Icm system intact). The first frames have an arrow pointing to the bacterium, which is tumbling in the extracellular medium. The bacterium then contacts the macrophage, and a large puff immediately forms starting at the site of bacterial contact. The puff then contracts and the video ends. The video ends before apparent internalization of the bacterium.

Video 3: DotA3. Shows a typical phagocytic response to a dotA mutant. The video begins with arrows pointing to a bacterium (LP03 *dotA*) tumbling in extracellular medium. Shortly after contact of the bacterium with the surface of the macrophage, a phase-dense ruffle appears that rapidly internalizes the bacterium. The video ends with the internalized bacterium out of the plane of focus of the lens and no longer visible. The size of the ruffle is smaller than witnessed for LP02, and the cellular material surrounding the bacterium is also considerably more phase dense than that seen for LP02. The images in Fig. 1 B of the attached manuscript are individual frames from this particular sequence.

Results

Diffuse Membrane Ruffles after Contact of Macrophages with L. pneumophila. Time-lapse phase-contrast videomicroscopy images captured in 2–3 s intervals throughout 10 min recording periods were used to follow the internalization of GFP-tagged *L. pneumophila* strains by A/J mouse bone marrow–derived macrophages (online supplemental video 2, titled "Ruffle (LP02)"; Fig. 1). After contact of macrophages with strains harboring an intact Dot/Icm system, large phase-transparent puffs extending along the plane of the coverslip were observed extending 5 μM or more in one direction outward from the site of initial bacterial contact with the macrophage (Fig. 1 A, large arrowhead; online supplemental video, and Fig. 1 A and G). The extension of the puffs often lasted for periods of >40 s before eventual retraction back to the site of bacterial binding (Fig. 1 A). Sometimes, there was no apparent internalization of the bacterium associated with the puff. Contact of a *dotA⁻* strain with the target macrophage, in contrast, resulted in much more circumscribed phase-opaque ruffles. These ruffles extended perpendicularly from the plane of the membrane, with the bacteria moving out of the focal plane of the site of bacterial binding, apparently signifying internalization underneath a phase opaque structure (Fig. 1 B, and online supplemental video 3, titled "DotA3").

It was difficult to acquire sufficient numbers of images to get significant comparisons between wild-type and mutant strains, so an alternative procedure was used to determine morphological changes induced in the macrophage after contact with *L. pneumophila*. To this end, bacteria were deposited onto macrophage monolayers by centrifugation, fixed either immediately, or after various incubation times at 37°C, and stained with phalloidin to detect actin filament
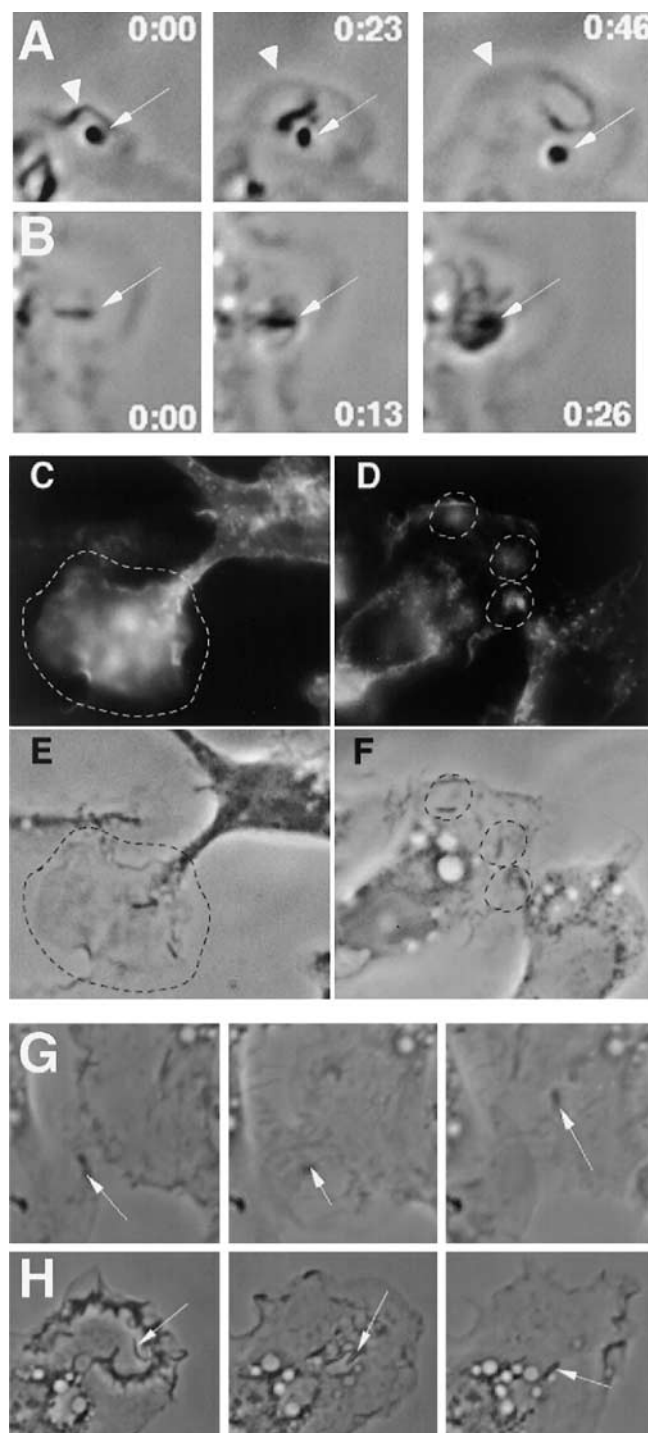

Figure 1. (A and B) Phase transparent puffs are associated with Dot/Icm-promoted uptake by macrophages. Displayed are images captured at various times after contact of *L. pneumophila* with macrophages. Times refer to seconds after leftmost image was captured. Thin arrows point to bacteria, whereas thick arrowheads point to expanding ruffles. (A) LP02 (intact Dot/Icm) observed after contact with macrophage. (B) LP03 (*dotA*) observed after contact with macrophage (online supplemental video titled "DOTA3"). (C–F) Diffuse ruffles and actin aggregation are dependent on an intact Dot/Icm system. Displayed are incubations of macrophages with LP02-GFP (C) and LP03-GFP (D) stained by phalloidin. Also shown are phase contrast micrographs of the identical microscope fields for LP02-GFP (E) and LP03-GFP (F). (G and H) Videomicroscopy of LP02-GFP introduced onto bone marrow macrophages. Supplemental online videos (G) "Ruffle (LP02)" and (H) "Macropin (LP02)."

formation microscopically (Materials and Methods). Immediately after depositing on the monolayer, the strain having an intact Dot/Icm system (LP02) showed diffuse actin ruffling about the site of bacterial binding, as observed by either phalloidin staining (Fig. 1 C, circled region) or phase microscopy (Fig. 1 E, circled region). The *dotA⁻* mutant (LP03) showed primarily small circumscribed regions of phalloidin staining at sites of binding (Fig. 1 D and F, circled regions). Immediately after centrifugation of the *dotA⁻* strain onto the macrophages, ∼40% of the bacteria were found associated with areas of tightly associated phalloidin staining. In contrast, only 5% of bacteria having an intact Dot/Icm system had similar tightly circumscribed actin structures that were limited to the contiguous sites of binding (data not shown).

Macropinocytosis and Retarded Uptake of L. pneumophila Is Dependent on dot/icm Genes. Based on analysis of time-lapse videomicroscopy, it appeared that after induction of diffuse ruffling, the microorganisms were internalized into large vacuoles that formed transiently (Fig. 1 H; online supplemental video 1, titled "Macropin (LP02)"). To analyze this further, samples were fixed after short incubations of A/J mouse macrophages with *L. pneumophila*. For LP02 (Dot/Icm system intact), the bacteria were found in large concentric vacuoles that were similar in morphology to fluid-filled macropinosomes (42). These structures were readily observed either by allowing the infection to proceed in the presence of the fluid-phase marker TRITC-Dextran, MW = 155 kD (Rh-Dx155; Fig. 2 A), or by phase contrast microscopy (Fig. 2 B). Macrophages incubated simultaneously with *L. pneumophila* and 1 mg/ml Rh-Dx155 accumulated the marker in large vacuoles containing bacteria (Fig. 2 A) whereas little marker accumulated in phagosomes harboring the *dotA⁻* strain although marker was sometimes found in vesicles nearby the phagosomes (LP03; Fig. 2 C). Similarly, phase contrast micro-
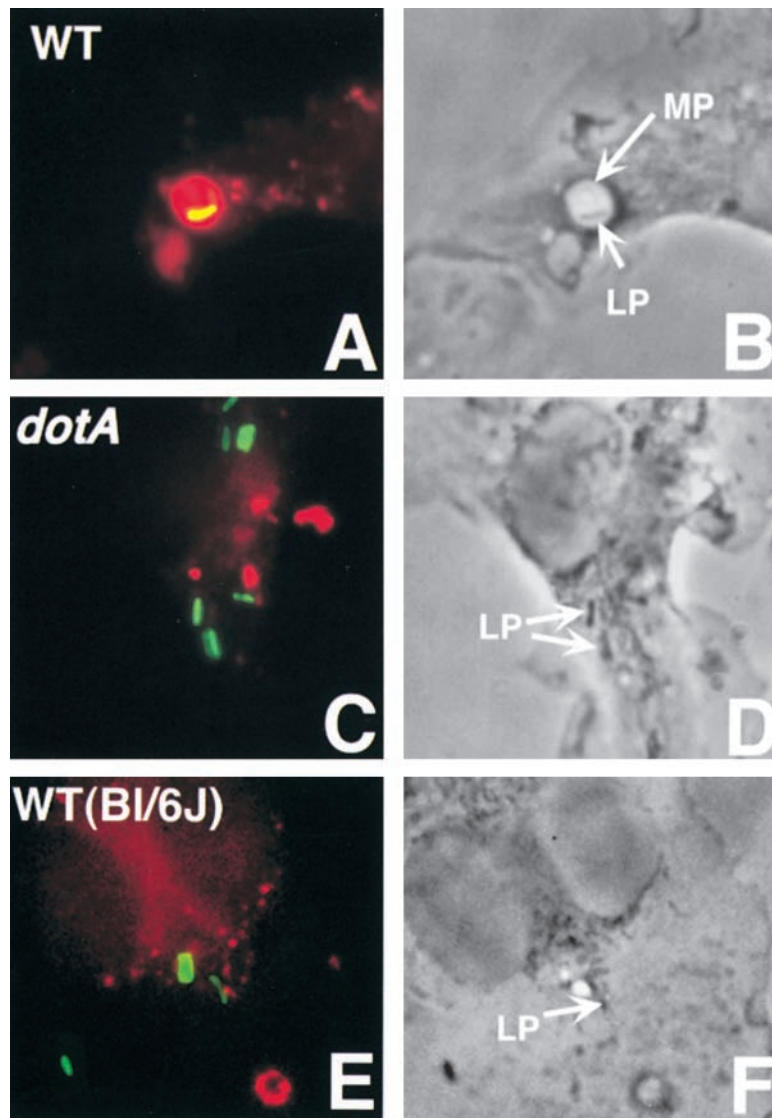

Figure 2. Macropinosome formation by *L. pneumophila.* Bone marrow–derived macrophages were incubated for 10 min at 37°C in the presence of GFP-expressing bacteria and Rh-Dx155, fixed, and processed for phase and immunofluorescence microscopy. Displayed are macrophages from A/J mice incubated with LP02 (Dot/Icm intact; A and B) or LP03 (*dotA*; C and D) as well as macrophages from C57Bl/6J mice incubated with LP02 (Dot/Icm intact; E and F). Shown are GFP and rhodamine channels merged (A, C, and E) or phase contrast images (B, D, and F). LP, *L. pneumophila*; MP, macropinosome.

graphs showed LP02 in large phase-transparent vacuoles (Fig. 2 B), whereas the *dotA⁻* mutant was found in considerably smaller compartments (Fig. 2 D). The presence of *L. pneumophila* in large vacuoles was dependent on incubation of bacteria with macrophages isolated from permissive strains of mice. Macrophages isolated from the C57Bl/6J mouse, which restrict *L. pneumophila* growth, showed little

ability to support the formation of these large vacuoles harboring *L. pneumophila* (Fig. 2 E and F; see below, Fig. 7). It was also noted that the number of internalized bacteria appeared significantly greater for the *dotA⁻* strain than for the strain harboring an intact Dot/Icm system (Fig. 3 A). As the morphology of the large vacuole was similar to a macropinosome, the term macropinosome will be used to refer to the large vacuoles.

The differences in the rate of phagocytosis and the formation of macropinosomes for wild-type and mutant organisms were quantitated microscopically at various times of incubation, using strategies that allowed as synchronous an infection as possible (Materials and Methods). If the bacteria were deposited onto macrophage monolayers by centrifugation, the *dotA* mutant was rapidly internalized, with most of the associated bacteria internalized before further incubation at 37°C (Fig. 3 A, white bar). In contrast, internalization of LP02 was significantly delayed and never attained the same levels of internalization as the mutant, at least when using centrifugation to establish bacterial contact (Fig. 3 A, black bar). In regards to macropinosome formation, by 10 min after centrifugation of LP02, >60% of the bacteria were found in large compartments containing Rh-Dx155 that could be detected easily by phase contrast microscopy (Fig. 3 B, black bar). The ability to observe macropinosomes decayed rapidly after this time point, with few bacteria costaining with Rh-Dx155 at 30 min after infection. Macropinosome formation appeared dependent on several of the Dot/Icm loci. In addition to the mutation in *dotA*, strains harboring in-frame deletions in *dotH*, *dotI*, and *dotO* all failed to form macropinosomes (data not shown).

Lowered phagocytosis rates and transient macropinosome formation were not dependent on a particular strategy of bacterial contact with the macrophage. Opsonization increased both the rate and total amount of uptake for each strain, (Fig. 3 C) but the total number of LP02 internalized was still less than that observed for the *dotA⁻* mutant (Fig. 3 C). In addition, the rate of appearance of Dot/Icm-dependent macropinosomes was enhanced by opsonization (Fig. 3 D), with macropinosomes surrounding ∼50% of the bacteria at the earliest timepoint analyzed
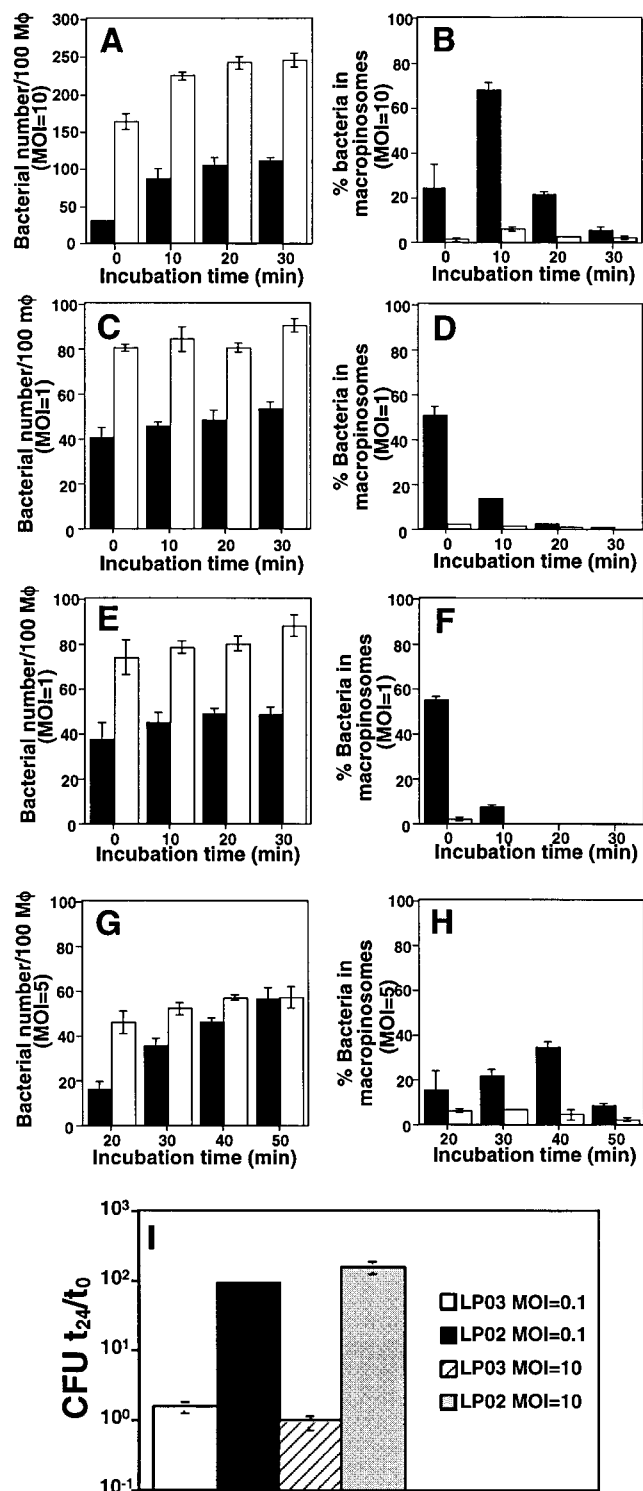

Figure 3. Delayed uptake and macropinosome formation promoted by the *L. pneumophila* Dot/Icm system. Black bar, LP02 (*dot/icm⁺*). White bar, LP03 (*dotA⁻*). Uptake (A, C, E, and G) or macropinosome formation (B, D, F, and H) were quantitated as described in Materials and Methods. Incubation periods were either after short centrifugation (A–F) or in the absence of centrifugation (G and H). (A and B) No opsonization. (C and D) Opsonization with anti-*L. pneumophila* serum (Materials and Methods). (A–D) Bacterial strains harbor GFP. (E–H) Bacterial strains harboring pAY68 (pH 6.0 Ag). 100 macrophages were examined per coverslip. Data are the mean of triplicate samples ± SE. MOI is indicated on the y axis. (I) Intracellular growth of *L. pneumophila* after infection at MOI = 10. *L. pneumophila* strains LP02 (intact Dot/Icm) or LP03 (*dotA⁻*) were introduced at MOI = 0.1 or 10 by centrifugation onto monolayers of A/J mouse bone marrow macrophages and assayed for increase in viable counts over a 24-h period (Materials and Methods). t_{24}/t_0 = bacterial counts at 24 h of incubation/bacterial counts determined after allowing for initial uptake of the bacteria (Materials and Methods).

(Fig. 3 D, black bar). As had been observed with unopsonized bacteria, the morphology of the vacuoles changed rapidly, since almost no macropinosomes were observed after 20 min of incubation (Fig. 3 D, black bar). The enhanced formation of macropinosomes by opsonization appeared to be a result of an increased efficiency of adhesion, rather than due to the bacteria binding to an opsonic receptor. *L. pneumophila* harboring the pH 6.0 antigen pilus from *Y. pseudotuberculosis* (31), which also enhanced adhesivity, gave results that were nearly identical with those observed for opsonized bacteria (Fig. 3 E and F). LP02 bearing the pH 6.0 antigen pilus showed similarly lowered total amount of uptake relative to the *dotA*⁻ strain (Fig. 3 E) and exhibited early transient macropinosome formation compared with the unopsonized control (Fig. 3 B and F). The presence of the pilus did not inhibit *L. pneumophila* intracellular replication (see Supplemental Online Data).

As each of the above conditions used centrifugution to synchronize the infection, which enhanced the ability to observe a clearly short-lived event ($t_{1/2} < 5$ min, Fig. 3 F), it was possible that depositing in this fashion could induce macropinosomes. Therefore, to study passively adherent bacteria in the absence of centrifugation, the pH 6.0 pilus-bearing strain was analyzed so that large numbers of bacteria could initiate uptake in a sufficiently short time period to observe transient macropinosome formation (Fig. 3 G and H). The results were similar to those observed using centrifugation, with a higher initial uptake rate for the *dotA*⁻ strain compared with LP02, although the overall amount of internalized bacteria after 50-min incubation eventually reached identical levels for these strains (Fig. 3 G). Similarly, Dot/Icm-dependent macropinosome formation could be detected after passive adhesion (Fig. 3 H), although the levels of macropinosomes observed were somewhat lower than in the presence of centrifugation (compare Fig. 3 F and H). Since the macropinosomes were so short-lived, an asynchronous infection is predicted to result in this lowered level of detection.

Several of the above experiments used MOI that were higher than normally used to monitor *L. pneumophila* replication (Figs. 3 B and G; 5 or 10 bacteria per target macrophage), so we wanted to demonstrate that the conditions that caused macropinosome formation also allowed intracellular growth. Using an MOI = 10, bacteria showed a large increase in intracellular viable counts after 24-h incubation that was indistinguishable from growth initiated after incubation using an MOI = 0.1 (Fig. 3 I). Therefore, the conditions used to analyze macropinosome formation also allowed efficient intracellular growth.

Macropinosome Formation Is the Result of Simultaneous Ingestion of Bacteria and Fluid Phase. Unopsonized *L. pneumophila* required incubation at 37°C for 10 min to observe maximal cointernalization of the fluid-phase marker (Fig. 3 B). One explanation for this delay in acquisition of the marker is that the bacterium is internalized into a phagosome that excludes Rh-Dx155, and then a fusion event takes place after internalization that results in transient expansion of the phagosome and introduction of the fluid phase marker.

To investigate the above possibility, macrophages were preloaded for 30 min with Rh-Dx155 before addition of *L. pneumophila*, and infection was allowed to proceed either in the presence or absence of the marker (Fig. 4). As expected, if the bacteria were added in the continued presence of the marker, colocalization of Rh-Dx155 with the Dot/Icm⁺ strain was very similar to that observed when there was no preincubation of Rh-Dx155 before infection (Fig. 4 A, gray bar). The behavior of the *dotA* mutant, however, was different than in the previous protocol (Fig. 4 A, black bar). At 20 min after infection, there was transient colocalization of Rh-Dx155 with the *dotA* mutant, implying that the marker accumulated in an intracellular compartment that could fuse with the mutant but not with the wild-type strain. If Rh-Dx155 were washed out of the medium before the addition of bacteria, colocalization of the marker with the Dot/Icm⁺ strain was almost completely lost (Fig. 4 B, gray bar). In contrast, removing the
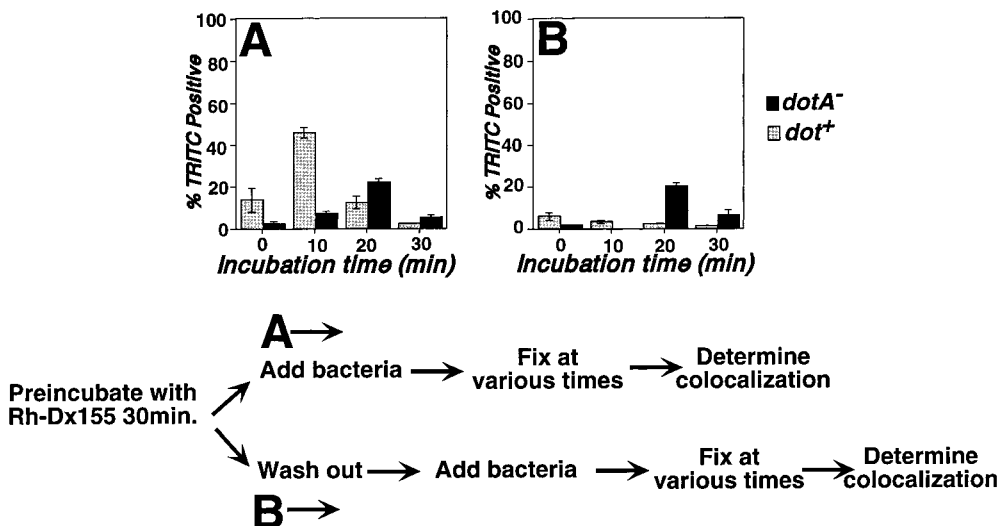

Figure 4. Compartments preloaded with a fluid-phase marker do not fuse with macropinosomes harboring *L. pneumophila* with intact Dot/Icm system. Bone marrow–derived macrophages were incubated at an MOI = 10 along with 1 mg/ml Rh-Dx155 for 30 min at 37°C and then incubated with bacteria either in the continued presence (A) or absence (B) of the fluid-phase marker (Materials and Methods). Number of bacteria in compartments staining with TRITC was determined as described in Material and Methods. Gray bar, LP02-GFP (intact Icm/Dot system); black bar, Lp03-GFP (*dotA*⁻).

fluid-phase marker before the addition of the *dotA* strain gave results that were similar to those observed with continued incubation of Rh-Dx155 during the infection, as there was transient colocalization of Rh-Dx155 with the phagosomes (Fig. 4 B, black square). These results are consistent with LP02 being simultaneously ingested with Rh-Dx155 into a fluid-filled phagosome that resists fusion with marker-filled compartments. In contrast, phagosomes harboring the *dotA* strain formed without simultaneous ingestion of Rh-Dx155, but were able to fuse with marker-filled compartments after internalization.

Sequestration of Macromolecules on Macropinosomes Bearing L. pneumophila. Previous work on *L. pneumophila* indicated that macrophage plasma membrane proteins are excluded from the vacuole (6, 43), but there is transient association of the small GTPase Rab7 in a fraction of the vacuoles (14, 44). To determine if the macropinosomes identified above behave similarly to replication vacuoles previously analyzed, the vacuoles were probed with a variety of reagents. Consistent with previous results (6), the transmembrane protein CD44 was found associated with ruffles in the plasma membrane above the vacuole, but was excluded from the *L. pneumophila*–bearing macropinosome (Fig. 5, CD44; Fig. 6 A and E). As had been reported for exclusion of transferrin receptor, there was little difference between a LP02 and a *dotA*⁻ strain (Fig. 6 A). The kinetics and degree of association of Rab7 with internalized bacteria from both bacterial strains was also similar to that reported previously, with maximal association of Rab7 occurring af-

ter 10-min incubation at 37°C (Fig. 5, Rab7; Fig. 6 B, reference 14). However, the association of Rab7 with internalized *L. pneumophila* was remarkably high if the analysis were limited to the observation of macropinocytotic vacuoles (Fig. 6 E). Greater than 70% of the macropinosomes bearing *L. pneumophila* were found to have associated Rab7, consistent with recruitment of this protein during, or shortly after, the formation of the vacuole (Fig. 6 E).

Similar to our results with CD44, a failure to detect localization of transmembrane proteins has been reported for newly formed parasitophorous vacuoles bearing *Toxoplasma gondii* (37). Components known to be associated with cholesterol–rich membrane rafts such as GM1 gangliosides and GPI-linked proteins, on the other hand, are internalized with the parasitophorous vacuole (37). To determine if formation of the *L. pneumophila* macropinosome involves a similar sorting process, infected macrophages were probed with reagents known to recognize the *T. gondii* parasitophorous vacuole. To this end, *L. pneumophila* and biotin-labeled CTB, which binds GM1-gangliosides, were simultaneously incubated with macrophages (Fig. 5 D, GM1). CTB was found to localize around the internalized *dot/icm*⁺ strain with kinetics of association similar to that observed for Rab7 (Fig. 6 C). In contrast, colocalization of CTB with the *dotA*⁻ strain was much less pronounced (Fig. 6 C). As was true for Rab7, if only the subset of bacteria found in macropinosomes were analyzed, 70% of the vacuoles were found to have cointernalized CTB and *L. pneumophila* (Fig. 6 E). The infected macrophages were also
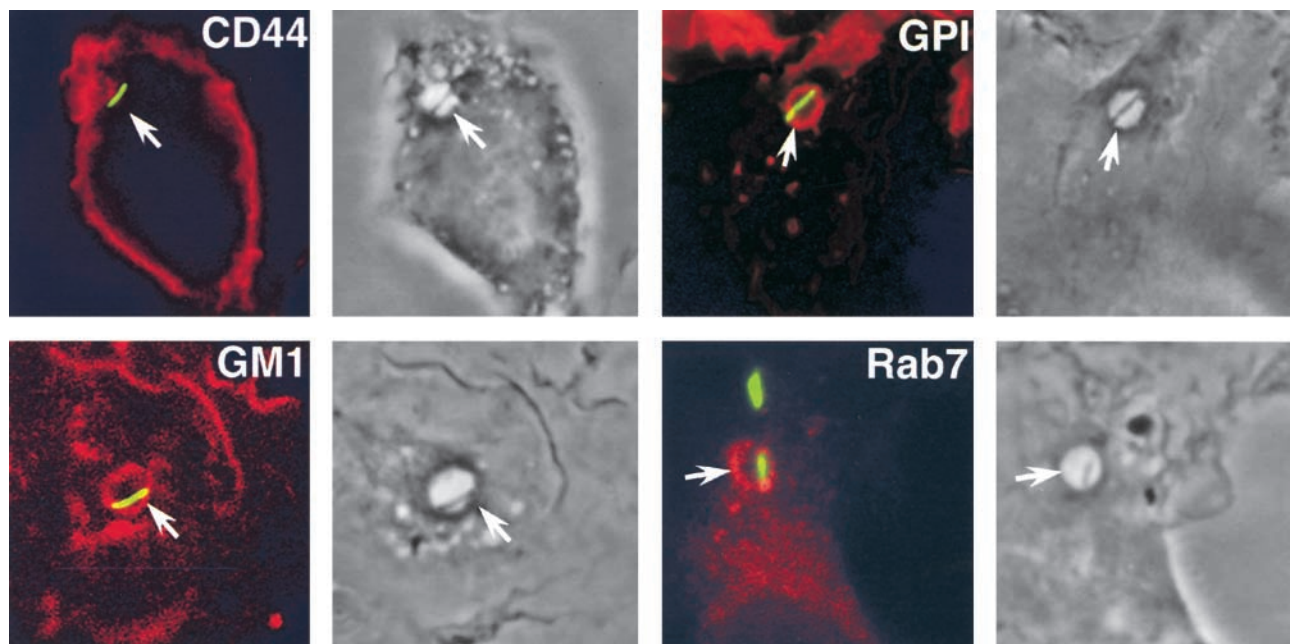

Figure 5. Association of membrane-localized markers with *L. pneumophila* macropinosomes. Bone marrow–derived macrophages were incubated with *L. pneumophila*, and membrane associated markers were localized by immunofluorescence, as described in Materials and Methods. Shown are merged images of the GFP and TRITC channels side-by-side with phase-contrast images of the identical cells. CD44, fixed cells probed with anti-CD44; GPI, fixed cells probed with Alexa594-aerolysin; GM1, cells coincubated with biotin-CTB subunit and bacteria (Materials and Methods); Rab7, fixed cells probed with anti-Rab7. Arrows, edge of phagosomal membranes.
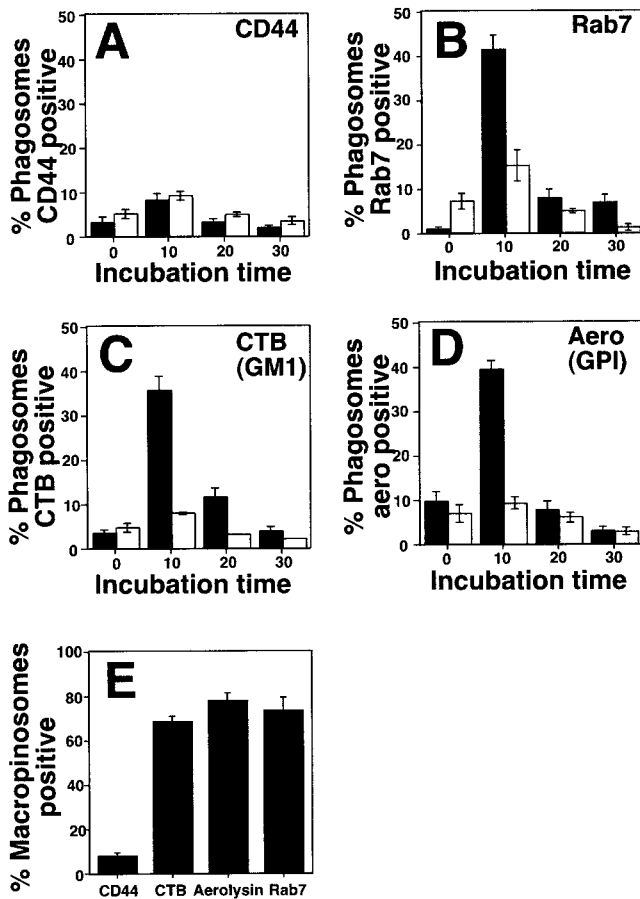
Figure 6. Kinetics of colocalization of membrane-associated markers with *L. pneumophila*-bearing phagosomes. (A–D) LP02-GFP (Dot/Icm intact) or LP03-GFP (*dotA*) at an MOI = 10 were centrifuged onto macrophage monolayers, then incubated for the noted periods of time at 37°C before fixation and probing with indicated reagents (Materials and Methods). "% phagosomes positive" refers to percentage of internalized bacteria that show costaining with the noted markers, based on observation of 100 bacteria per coverslip (Materials and Methods). The data represent the mean ± SE of three coverslips. (E) Macrophages incubated with LP02-GFP for 10 min at 37°C were probed for noted markers, and macropinosomes harboring GFP-labeled bacteria were identified by fluorescence and phase microscopy. The macropinosomes were then observed for the presence of the noted markers, as in A–D. "% positive" refers only to those phagosomes with a macropinocytotic morphology, and represents percentage of macropinosomes that show costaining with the noted markers. Data for macropinosomes are from triplicate coverslips representing 50 macropinosomes per coverslip. CD44, anti-CD44; Aero, Alexa594-aerolysin; Rab7, anti-Rab7. Black bar, LP02 (Dot/Icm intact); white bar, LP03 (*dotA*).

probed with Alexa594-aerolysin (Fig. 5, GPI), which binds to the GPI moiety of GPI-linked membrane proteins (45, 46). The kinetics of association of GPI-linked proteins, based on this assay, was almost identical to that observed for CTB colocalization (Fig. 6 D), with the staining of the vacuoles being remarkably intense (Fig. 5, GPI). As was true for CTB and Rab7, if only *L. pneumophila*-bearing macropinosomes were analyzed, colocalization was abundant, with close to 80% of the vacuoles staining with aerolysin (Fig. 6 E). Therefore, differential sorting of plasma membrane proteins seems to occur in a fashion similar to that observed previously for *T. gondii* (37).

Host-specific Restriction of L. pneumophila Growth Is Associated with an Inability to Form Macropinosomes. Based on the above results, *L. pneumophila* is obviously stimulating factors within the macrophage to promote a special internalization route. Very little has been established regarding which host factors could be involved at any step in the formation of the replication vacuole, other than genetic data from RI mouse strains. As the ability to form macropinosomes appears highly correlated with the ability to initiate intracellular replication, it was of particular interest to determine if the *Lgn1* allele that restricts intracellular growth acts at the level of macropinosome formation by *L. pneumophila*.

Macrophages from the restrictive C57BL/6J internalized *L. pneumophila* Dot/Icm+ or *dotA*− strains at identical efficiencies (Fig. 7 A), in distinct contrast to what was observed previously for macrophages from A/J mice (Fig. 3 A). These internalization profiles were similar to what was seen for the *dotA*− strain incubated with A/J mouse-derived macrophages (Fig. 3 A), consistent with obstruction of a Dot/Icm-dependent uptake pathway in C57BL/6J macrophages. In support of this interpretation, there was a total absence of macropinosome formation by *L. pneumophila* within bone marrow macrophages derived from C57BL/6J mice (Figs. 2 E and F, and Fig. 7 B). Again, in the C57BL/6J mouse, the Dot/Icm+ strain behaved similarly to a *dotA*− strain (Figs. 7 B and 3 B, white bar).

To further confirm the connection between restriction of intracellular growth by C57BL/6J and an inability to promote early events associated with productive intracellular infection by *L. pneumophila*, macrophages from this strain were compared with those from the A/J mouse in two different assays. First, an assay alternative to the microscopic analysis was used to assess relative amounts of uptake in the two mouse strains (Fig. 7 C and D). By assaying for viable counts protected from gentamicin killing in macrophages from the A/J mouse, a slower uptake rate was observed for the Dot/Icm+ strain relative to the *dotA*− strain (Fig. 7 C), and this difference was eliminated in macrophages from C57BL/6J (Fig. 7 D). Second, the ability of *L. pneumophila* to evade trafficking into the endosomal pathway was measured in macrophages from these two mouse strains, scoring for acquisition of LAMP-1. As reported previously (36), >80% of the phagosomes containing LP02 failed to colocalize with LAMP-1 in macrophages from A/J mice after 10–30-min incubation at 37°C (Fig. 7 E, black bar), whereas the *dotA*− strain was found predominantly colocalized with LAMP-1 (Fig. 7 E, white bar). In contrast, after 10-min incubation at 37°C, >80% of the bacteria from both strains were found to be colocalized with LAMP-1 in macrophages from C57BL/6J (Fig. 7 F). Therefore, an inability of macrophages from C57BL/6J mice to support macropinocytotic uptake of *L. pneumophila* correlated with an inability of the phagosome to avoid interaction with endocytic pathway.

Introduction of *L. pneumophila* at high MOI onto macrophage causes rapid cytotoxicity of the target cells (34), so
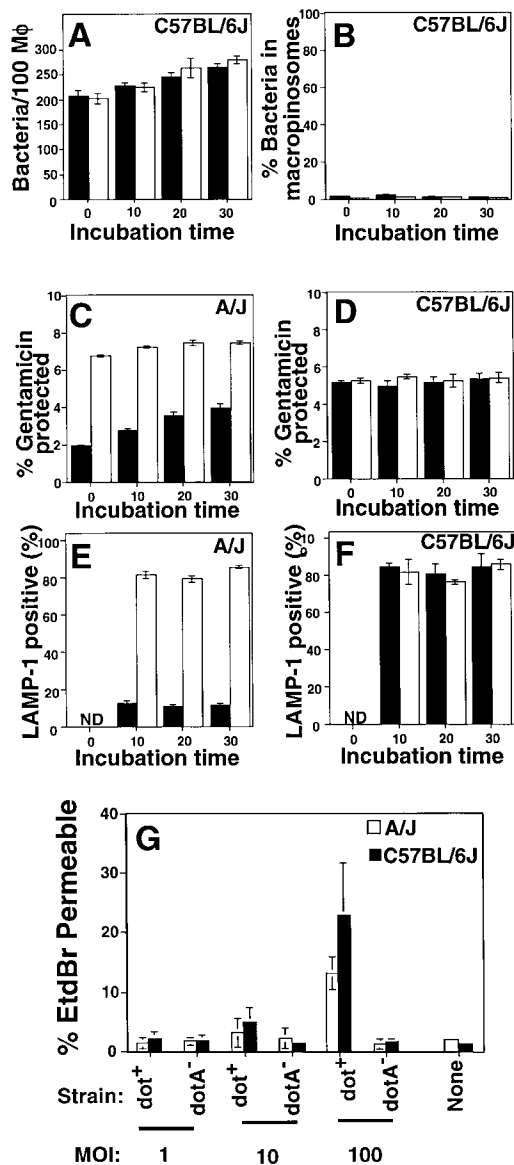
Figure 7. Defective targeting and macropinosome formation in the Lgn-restrictive strain C57Bl/6J. Bone marrow–derived macrophages were isolated from either C57Bl/6J or A/J mice and challenged with either LP02-GFP (black bar, intact Dot/Icm) or LP03-GFP (white bar, *dotA*−; Materials and Methods). In A and B, the MOI = 10 bacteria/macrophage. In C–F, the MOI = 1.0 bacteria/macrophage. (A) Uptake efficiency by C57Bl/6J macrophages was determined by antibody probing, as in Fig. 3. (B) Macropinosome formation by C57Bl/6J macrophages was determined by colocalization of bacteria with Rh-Dx155, as in Fig. 3. (C and D) Uptake efficiency by A/J (C) and C57BL/6J (D) macrophages was determined by protection of internalized bacteria from gentamicin killing (reference 34). (E and F) Ability of *L. pneumophila* to bypass entry into the endocytic pathway was determined by indirect immunofluorescence probing of fixed samples with anti–LAMP-1 (reference 36). Colocalization of LAMP-1 with bacteria was determined for bone marrow macrophages derived from A/J (E) or C57BL/6J mice (F). ND, no colocalization detectable. Data are mean of triplicate coverslips ± SE, 100 bacteria per coverslip. (G) Macropinosome formation in permissive macrophages is not the result of enhanced cytotoxicity. Coverslips of macrophages from either A/J or C57BL/6J mice were incubated at the indicated MOI with either LP02 (*dot*+) or LP03 (*dotA*−) and assayed for cytotoxicity by enumerating EtdBr-permeable cells microscopically (Materials and Methods; reference 34). Cytotoxicity or percentage of EtdBr permeable equals the percentage of cells found to be EtdBr permeable in rhodamine fluorescence channel relative to total number of cells on coverslip (Materials and Methods).

it is possible that macropinosome formation was the result of a cytotoxic response that occurs in macrophages derived from A/J but not C57Bl/6 mice. Therefore, macrophages from both strains were challenged with *L. pneumophila* at various MOI, and death of macrophages was determined 60 min after centrifugation of the bacteria onto the monolayers (Materials and Methods). There was little difference in the amount of cytotoxicity observed in macrophages from the two strains at the MOI used in this study (Fig. 7 G; MOI = 1 or 10). In fact, the amount of death at MOI = 10 was far less than the number of macropinosomes formed in macrophages from the A/J mouse. At a higher MOI, there was somewhat more cytotoxicity observed for the C57Bl/6 compared with A/J macrophages (Fig. 7 G), arguing against large vacuole formation being a cytotoxic response elicited by A/J macrophages.

The Defect in Promoting Macropinosome Formation by C57BL/6J Mice Cosegregates with the Lgn1 Locus. It was next determined whether the ability to block macropinosome formation in C57BL/6J mapped to *Lgn1*. RI strains exist that are crosses between A/J and C57BL/6J, and macrophages from many of these strains have been characterized for the ability to support *L. pneumophila* replication (47). These RI strains allow the inheritance patterns of phenotypes and markers to be correlated (21).

A panel of 10 RI strains were chosen to characterize further, and the genotypes of these strains were determined for an extensive set of DNA polymorphisms that map to the *Lgn1* region (24). The haplotypes of each of these strains were consistent with their previously determined ability to support or restrict *L. pneumophila* intracellular replication (Table I, *Lgn1* haplotype; Materials and Methods, reference 47). The PCR products for three of the markers located internally to the *Lgn1* locus are displayed (D13Die6, D13Die36-A,B, and D13Die3) in addition to the STS marker map, to demonstrate that restrictive strains have the polymorphisms found in the C57BL/6J mouse and permissive strains have the polymorphisms found in A/J mice (Fig. 8).

Bone marrow–derived macrophages from each of the 10 RI strains were then analyzed for internalization of *L. pneumophila* as well as the ability of *L. pneumophila* to undergo macropinocytotic uptake and avoid fusion of the vacuole with a LAMP-1–containing compartment (Table I). All the strains, except one, behaved phenotypically in a manner that was predicted by their *Lgn1* haplotype, as the macrophages from strains having the C57BL/6J haplotypes could not support Dot/Icm-dependent events such as macropinosome formation, while those with the A/J haplotype could (Table I). The one exception to this pattern was strain A×B-5 (A/J haplotype), which did not behave precisely like either the A/J or C57BL/6J parents. The number of Dot/Icm-dependent macropinosomes formed per macrophage was similar for A/J and A×B-5 (Table I; macropinosomes per 100 macrophages) and there were high levels of avoidance of LAMP-1 compartments for A×B-5. The total uptake of *L. pneumophila* by macrophages from A×B-5, however, was close to three times greater than

Table I. *Macropinosome Formation Is Blocked by the Restrictive Lgn1 Allele*

Mouse strain	Intracellular growth[a]	Lgn1[b] haplotype	Bacterial strain[c]	Macropinosomes/ 100 macrophages	Macropinosome formation[d]	Uptake[d]	LAMP-1–positive[e]
					(%)		(%)
A/J	P	A/J	WT	58 ± 3	53 ± 2.4	110 ± 5.9	12 ± 1.8
			dotA	6 ± 1	3.6 ± 0.4	182 ± 11	80 ± 1.2
A×B-2	P	A/J	WT	62 ± 1	52 ± 0.9	118 ± 3.6	13 ± 1.5
			dotA	10 ± 3	5.1 ± 1.4	193 ± 13	79 ± 2.5
A×B-5	P	A/J	WT	54 ± 3	19 ± 1.4	288 ± 16	50 ± 4.2
			dotA	17 ± 2	6.7 ± 0.8	258 ± 7.1	82 ± 0.94
A×B-6	R	B6	WT	8 ± 1	4.8 ± 0.2	173 ± 11	79 ± 0.7
			dotA	7 ± 2	4.0 ± 1.1	175 ± 5.3	81 ± 0.5
A×B-10	R	B6	WT	11 ± 1	6.2 ± 0.3	172 ± 11	79 ± 1.2
			dotA	8 ± 2	4.8 ± 1.4	173 ± 5.6	80 ± 1.4
A×B-12	P	A/J	WT	54 ± 3	52 ± 2.7	104 ± 4.6	12 ± 0.6
			dotA	10 ± 2	4.9 ± 0.9	193 ± 5.4	79 ± 1.4
B×A-7	R	B6	WT	16 ± 2	7.4 ± 0.7	216 ± 27	73 ± 1.7
			dotA	10 ± 1	4.9 ± 0.4	199 ± 21	80 ± 1.7
B×A-8	R	B6	WT	8 ± 2	4.9 ± 1.4	166 ± 2.7	76.7 ± 1.7
			dotA	8 ± 2	4.6 ± 1.4	176 ± 4.4	79 ± 2.4
B×A-13	R	B6	WT	5 ± 1	3.3 ± 0.4	146 ± 11	78 ± 3.8
			dotA	6 ± 1	3.3 ± 0.4	168 ± 6.3	78 ± 2.3
B×A-14	P	A/J	WT	42 ± 1	53 ± 1.0	79 ± 12	12 ± 1.3
			dotA	6 ± 2	3.9 ± 1.4	160 ± 13	81 ± 1.9
B×A-26	R	B6	WT	7 ± 1	4.0 ± 0.6	180 ± 2.5	81 ± 1.7
			dotA	10 ± 1	6.0 ± 0.4	177 ± 3.3	80 ± 0.5

[a]P, permissive for intracellular growth; R, restrictive for intracellular growth. Data from reference 47.
[b]All strains have been analyzed for the following STS markers (Materials and Methods): D13Mit146, D13Die6, D13Die26, D13Die7B, D13Die36A, D13Die25D, D13Die7A, D13Die36B, D13Die3, and D13Die73 (reference 38).
[c]dotA, Lp03-GFP; WT, LP02-GFP.
[d]Uptake and macropinosome formation determined as described in Fig. 3 A and B, respectively.
[e]Percentage of LAMP-1–positive determined as described in Fig. 8.

that found for the A/J strain and, in fact, was greater than even the RI strains having the C57BL/6J haplotype (Table I). This increased uptake resulted in a lower efficiency of macropinosome formation and avoidance of a LAMP-1 compartment per cell-associated bacterium for this strain relative to A/J (Table I). We interpret these data as indicating that A×B-5 has a phenotype that is permissive for macropinosome formation and LAMP-1 avoidance (A/J-like, as predicted by its haplotype). An unrelated genetic event, however, presumably caused an increase in a parallel uptake path in this RI strain that resulted in formation of phagosomes that fused with LAMP-1–containing compartments.

A strain distribution pattern (SDP) for macropinosome formation was created, using the interpretation that A×B-5 is permissive for macropinosome formation, and this was analyzed for linkage in the RI strain set using Map Manager 2.6.5 (http://mcbio.med.buffalo.edu/mapmgr.html). The macropinosome strain distribution pattern was linked to chromosome 13 near Lgn1 at the 99% limit of linkage

evaluation. No other loci were linked at this threshold. Therefore, intracellular growth, macropinocytotic uptake, and avoidance of a LAMP-1 compartment are all highly dependent on having both an intact Dot/Icm system and an appropriate Lgn1 allele. Both Dot/Icm and the Lgn1 allele control extremely early steps in the L. pneumophila replication cycle.

Discussion

It has been reported that uptake of L. pneumophila occurs via coiling phagocytosis in which a single pseudopod wraps around the bacterium (7, 48). In this communication, we have presented data that L. pneumophila strains competent for replication vacuole formation induce an uptake process that is morphologically distinct from that promoted by strains having a defective Dot/Icm apparatus and is apparently unrelated to coiling phagocytosis. These results are consistent with the model that Dot/Icm forms an apparatus
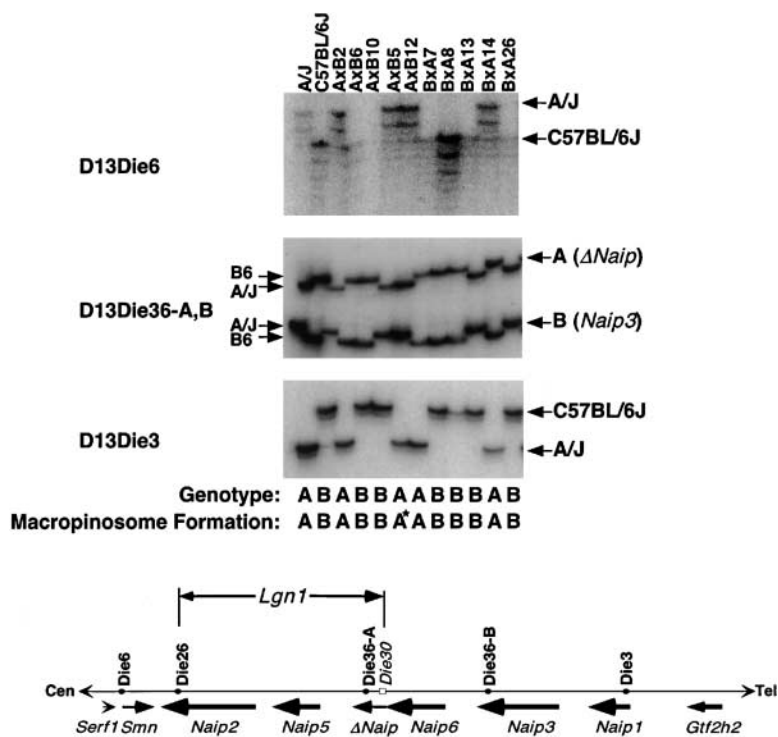
Figure 8. RI strains having STSs of C57Bl/6J do not support *L. pneumophila* macropinosome formation. Displayed is polyacrylamide gel of PCR analysis of three STSs located within the *Lgn1* interval (D13Die6, D13Die36-A,B, and D13Die3), using DNA prepared from A/J, C57Bl/6J, and A×B RI strains (Materials and Methods). Arrows next to gel note bands corresponding to A/J or C57Bl/6J (also called B6) genotypes. Below the gel is the genotype of each strain, as determined by this analysis (A, *Lgn1* locus of A/J; B, *Lgn1* locus of C57Bl/6J). Asterisk refers to RI strain that has both high levels of macropinosome formation and high levels of uptake. Macropinosome formation is from Table I. Below the gel is the chromosomal location of each STS relative to the *Lgn1* locus.

that is involved in inducing a unique uptake path that results in avoidance of the lysosomal network and formation of a transient macropinosome. This is consistent with the proposition that the primary function of Dot/Icm is to deposit an effector molecule that directs the internalization route of externally bound bacterium.

Macropinosome formation has been documented with other pathogens. Internalization of *Salmonella typhimurium* by cultured macrophages is accompanied by macropinosome formation, and the presence of bacteria in this compartment correlates with the ability of the microorganism to survive intracellular killing mechanisms (49). It had been proposed that such "spacious phagosomes" enhance bacterial survival by slowing the rate of acidification or interfering with host antimicrobial defense mechanisms that work optimally in the smaller volume of a tight-fitting phagosome. The role of the *L. pneumophila* macropinosome in vacuolar trafficking, however, may be different from that of *S. typhimurium*. In the case of *L. pneumophila*, macropinosomes were induced transiently and shrank rapidly, with the majority of vacuoles appearing tightly apposed against the bacterial surface within 5 min after their initial appearance (Fig. 3 B). *S. typhimurium* macropinosomes, in contrast, persist within macrophages for longer periods of time than we observed with *L. pneumophila* (49). In fact, a serotype of *Salmonella* that promotes the formation of a rapidly shrinking compartment is significantly more sensitive to macrophage killing than serotypes that persist in the spacious compartment (50).

Previous work demonstrated that macrophage CSF and PMA stimulate both ruffling and macropinocytosis in macrophages within a few minutes after addition of these re-

agents (42, 51). In the case of nonopsonized *L. pneumophila*, macropinosome formation appeared delayed compared with uptake (Fig. 3 B). One explanation for this delay is that uptake of *L. pneumophila* produces a tight phagosome that subsequently expands as a result of fusion with other compartments. Our results argue against this possibility, as only a *dotA* strain was found in a phagosome that fused with preexisting compartments (Fig. 4 B). It is more likely that this delay in macropinosome formation is due to the preferential uptake of bacteria that fail to target into replicative vacuoles. We consistently find that ∼15% of internalized bacteria target improperly into a LAMP-1$^+$ compartment, so it is expected that this fraction of the bacteria will not be found in macropinosomes. Furthermore, at the earliest timepoints, uptake of bacteria that route into a LAMP-1–containing compartment is more than fivefold higher than that seen for bacteria having an intact Dot/Icm system (Fig. 3 A, compare uptake at 0 min of *dotA*$^−$ strain with LP02). Therefore, a large proportion of the intracellular bacteria at the 0 min timepoint are not internalized into replication vacuoles, but are instead destined to be routed into a LAMP-1–containing compartment. Consistent with this hypothesis is the fact that if the uptake efficiency of *L. pneumophila* via Dot/Icm is enhanced by opsonization or production of pili, then no delay is observed, and maximal macropinosome formation is seen immediately after centrifugation (Fig. 3 D and F).

The inability to observe fusion of the *L. pneumophila* vacuole with intracellular compartments preloaded with a fluid-phase marker is consistent with the macropinosome being formed during uptake of the bacterium, rather than as a post uptake fusion event (Fig. 4 B). The one major ca-

veat to this interpretation is that not all compartments within the macrophage may be loaded efficiently by the fluid-phase marker. If the *L. pneumophila* macropinosome involves fusion of material derived from the macrophage secretory pathway with the plasma membrane, labeling of the vacuole may not have been detectable using the preloading strategy described here.

Tethering the bacteria to the target cells by antibody opsonization did not interfere with the ability of the Dot/Icm system to promote macropinosome formation, and phagocytosis was still retarded relative to a similarly treated *dotA* strain. This implies that the phagocytic receptor bound by the bacterium has little influence on the uptake route of this microorganism, a result predicted by previous work showing that antibody-coated *L. pneumophila* grow efficiently within monocytes (18). Presumably, the effectors produced by the Dot/Icm system are able to override signals produced by phagocytic receptors, such as Fc receptors, which might otherwise route the phagosome into a lysosomal network. The power and flexibility of the Dot/Icm system in this regard is consistent with the fact that the organism is able to grow in a wide variety of cell types, including amoebae.

As observed previously, *L. pneumophila*-containing compartments excluded a type I transmembrane protein and were transiently associated with Rab7 (14, 43, 44). By restricting observations to only those vacuoles having a macropinocytotic morphology, the percentage of *L. pneumophila* compartments that have associated Rab7 is considerably higher than previously thought (Fig. 6). The extremely early association of the vacuole with Rab7 suggests that this protein may localize at this site during the formation of the macropinosome, a surprising result given that Rab7 is involved in the maturation of endosomes into late endosomal and lysosomal compartments (52). As *L. pneumophila* actively avoids these compartments, it is highly doubtful that association of Rab7 with the macropinosome has any functional importance. In fact, dominant inhibitory and constitutively active forms of Rab7 have consistently resulted in no negative affects on *L. pneumophila* growth (44; unpublished data). Perhaps some aspect of the macropinosome resembles the poorly characterized compartment that normally harbors Rab7, resulting in transient association of this protein.

It now appears that if the analysis is confined to *L. pneumophila* vacuoles having the morphology of macropinosomes, membrane-associated proteins are not completed excluded, in contrast to earlier results (43). As previously observed for vacuoles formed shortly after *T. gondii* uptake (37), the *L. pneumophila* macropinosome is studded with GPI-linked proteins. GPI-linked proteins appear to be associated with cholesterol-rich microdomains or detergent-insoluble rafts in the membrane, particularly after receptor clustering. Since another raft-associated marker, GM1 gangliosides (53), sequesters with the macropinosome, formation of the *L. pneumophila* macropinosome may involve selective retention of plasma membrane proteins and exclusion of others. Macropinocytotic uptake of the GPI-linked protein CD14 involves association with detergent-insoluble membrane microdomains, so there may be a common mechanism for macropinocytotic uptake (54). Several pathogens that avoid intracellular killing mechanisms appear to be internalized via paths that involve at least transient association with raft-associated proteins (55–58). It has been argued that raft-associated uptake processes may lead micoorganisms into compartments that avoid fusion with the lysosomal network (59).

Efficient macropinosome formation by a strain having an intact Dot/Icm system could only be observed in macrophages from RI mouse strains that had the *Lgn1* allele of A/J mice, and strains having the *Lgn1* allele of C57BL/6J showed lowered macropinocytotic uptake. Effectively, the restrictive *Lgn1* allele makes *L. pneumophila* behave as if it were lacking the Dot/Icm system. The restrictive *Lgn1* allele is dominant (21, 22), so assuming heterozygote mice do not suffer from a haploinsufficiency of the permissive allele, it seems likely that the restrictive allele either poisons the activity of the Dot/Icm system, or interferes with the product of the permissive *Lgn1* allele. The primary difference between permissive and restrictive strains is that C57BL/6J-derived peritoneal macrophages express higher levels of *Naip* transcripts (presumably primarily *Naip2*) than do A/J macrophages (60). It has also been demonstrated that *Naip* transcription is upregulated by phagocytosis, but it is highly unlikely this response plays any role in restricting *L. pneumophila* macropinosome formation. We observe macropinosome formation with much faster kinetics than the published upregulation of *Naips*, so the events we are observing are taking place long before transcription of *Naips* can be activated.

Similar host restriction has been observed for macropinosome formation induced by the *Salmonella* species (50). In the case of mouse strains in which there is little formation of these structures, it appears that there is a transient spacious compartment which rapidly shrinks. Furthermore, the mouse strains that support formation of a stable *Salmonella* spacious phagosome are different than those observed in this study. C57BL/6 and Balb/c allow efficient spacious phagosome formation by *S. typhimurium* (50), whereas these strains restrict *L. pneumophila* (C57BL/6, Fig. 7; Balb/c, data not shown), accentuating the presumed differences in the mechanisms of formation of these compartments by the two pathogens.

Although *L. pneumophila* is able to induce apoptosis (4), its connection to Naip control of intracellular growth is unknown. The kinetics of macropinosome formation are inconsistent with apoptosis inhibition by Naips playing a role in modulating *L. pneumophila* intracellular growth, since the affect of *Lgn1* on *L. pneumophila* growth appears to be exerted within seconds after bacterial contact. It seems more probable that the responsible Naip encoded by the *Lgn1* locus is able to regulate a *L. pneumophila*-promoted signaling event from the macrophage surface, and this signaling event may share intermediates that are involved in induction of, or interference with, an apoptotic program. Presumably, *Lgn1* modulates intracellular growth

by interacting with the Dot/Icm signaling pathway in some fashion. Alternatively, the host signaling pathway that is in contact with Dot/Icm is missing in mice having the restrictive *Lgn1* allele. Future work should be directed toward identifying these potential connections.

References

1. Nash, T.W., D.M. Libbey, and M.A. Horowitz. 1984. Interaction between the Legionnaires' disease bacterium (*Legionella pneumophila*) and human alveolar macrophages. *J. Clin. Invest.* 74:771–782.

2. Fields, B.S., G.N. Sanden, J.M. Barbaree, W.E. Morrill, R.M. Wadowsky, E.H. White, and J.C. Feeley. 1998. Intracellular multiplication of *Legionella pneumophila* in an amoebae isolated from hospital hot water tanks. *Curr. Microbiol.* 18: 131–137.

3. Wadowsky, R.M., L.J. Butler, M.K. Cook, S.M. Verma, M.A. Paul, B.S. Fields, G. Keleti, J.L. Sykora, and R.B. Yee. 1988. Growth-supporting activity for *Legionella pneumophila* in tap water cultures and implication of hartmannellid amoebae as growth factors. *Appl. Environ. Microbiol.* 54:2677–2682.

4. Gao, L.Y., and Y. Abu Kwaik. 1999. Apoptosis in macrophages and alveolar epithelial cells during early stages of infection by *Legionella pneumophila* and its role in cytopathogenicity. *Infect. Immun.* 67:862–870.

5. Cianciotto, N., B.I. Eisenstein, and N.C. Engelberg. 1989. Genetics and molecular pathogenesis of *Legionella pneumophila*, an intracellular parasite of macrophages. *Mol. Biol. Med.* 6:409–424.

6. Clemens, D.L., and M.A. Horowitz. 1995. Characterization of the *Mycobacterium tuberculosis* phagosome and evidence that phagosomal maturation is inhibited. *J. Exp. Med.* 181:257–270.

7. Horwitz, M.A. 1984. Phagocytosis of the Legionnaires' disease bacterium (*Legionella pneumophila*) occurs by a novel mechnism: engulfment within a pseudopod coil. *Cell.* 36:27–33.

8. Horwitz, M.A. 1983. The Legionnaires' disease bacterium (*Legionella pneumophila*) inhibits phagosome-lysosome fusion in human monocytes. *J. Exp. Med.* 158:2108–2126.

9. Swanson, M.S., and R.R. Isberg. 1995. Association of *Legionella pneumophila* with the macrophage endoplasmic reticulum. *Infect. Immun.* 63:3609–3620.

10. Sturgill-Koszycki, S., and M.S. Swanson. 2000. *Legionella pneumophila* replication vacuoles mature into acidic, endocytic organelles. *J. Exp. Med.* 192:1261–1272.

11. Segal, G., M. Purcell, and H.A. Shuman. 1998. Host cell killing and bacterial conjugation require overlapping sets of genes within a 22-kb region of the *Legionella pneumophila* genome. *Proc. Natl. Acad. Sci. USA.* 95:1669–1674.

12. Segal, G., and H.A. Shuman. 1999. Possible origin of the *Legionella pneumophila* virulence genes and their relation to *Coxiella burnetii*. *Mol. Microbiol.* 33:669–670.

13. Vogel, J.P., H.L. Andrews, S.K. Wong, and R.R. Isberg. 1998. Conjugative transfer by the virulence system of *Legionella pneumophila*. *Science.* 279:873–876.

14. Roy, C.R., K.H. Berger, and R.R. Isberg. 1998. *Legionella pneumophilia* DotA protein is required for early phagosome trafficking decisions that occur within minutes of bacterial untake. *Mol. Microbiol.* 28:663–674.

15. Wiater, L.A., K. Dunn, F.R. Maxfield, and H.A. Shuman. 1998. Early events in phagosome establishment are required for intracellular survival of *Legionella pneumophilia*. *Infect. Immun.* 66:4450–4460.

16. Coers, J., C. Monahan, and C.R. Roy. 1999. Modulation of phagosome biogenesis by *Legionella pneumophila* creates an organelle permissive for intracellular growth. *Nat. Cell. Biol.* 1:451–453.

17. Rechnitzer, C., and J. Blom. 1989. Engulfment of the Philadelphia strain of *Legionella* pneumophila within pseudopod coils in human phagocytes. Comparison with other *Legionella* strains and species. *APMIS.* 97:105–114.

18. Horwitz, M.A., and S.C. Silverstein. 1981. Interaction of Legionnaires' disease bacterium (*Legionella pneumophilia*) with human phagocytes. II. Antibody promotes binding of *L. pneumophilia* to monocytes but does not inhibit intracellular multiplication. *J. Exp. Med.* 153:398–406.

19. Payne, N.R., and M.A. Horowitz. 1987. Phagocytosis of *Legionella pneumophilia* is mediated by human monocyte complement receptors. *J. Exp. Med.* 166:1377–1389.

20. Venkataraman, C., B.J. Haack, S. Bondada, and Y. Abu Kwaik. 1997. Identification of a Gal/GalNAc lectin in the protozoan *Hartmannella vermiformis* as a potential receptor for attachment and invasion by the Legionnaires' disease bacterium. *J. Exp. Med.* 186:537–547.

21. Dietrich, W.F., D.M. Damron, R.R. Isberg, E.S. Lander, and M.S. Swanson. 1995. *Lgn1*, a gene that determines susceptibility to *Legionella pneumophilia*, maps to mouse chromosome. *Genomics.* 26:443–450.

22. Beckers, M.C., S. Yoshida, K. Morgan, E. Skamene, and P. Gros. 1995. Natural resistance to infection with *Legionella pneumophila*: chromosomal localization of the Lgn1 susceptibility gene. *Mamm. Genome.* 6:540–545.

23. Miyamoto, H., K. Maruta, M. Ogawa, M.C. Beckers, P. Gros, and S. Yoshida. 1996. Spectrum of *Legionella* species whose intracellular multiplication in murine macrophages is genetically controlled by Lgn1. *Infect. Immun.* 64:1842–1845.

24. Growney, J.D., and W.F. Dietrich. 2000. High-resolution genetic and physical map of the L*gn1* interval in C57BL/6J implicates Naip2 or Naip5 in *Legionella pneumophilia* pathogenesis. *Genome Res.* 10:1158–1171.

25. Yaraghi, Z., E. Diez, P. Gros, and A. MacKenzie. 1999. cDNA cloning and the 5′ genomic organization of Naip2, a candidate gene for murine *Legionella* resistance. *Mamm. Genome.* 10:761–763.

26. Deveraux, Q.L., and J.C. Reed. 1999. IAP family proteins-suppressors of apoptosis. *Genes Dev.* 13:239–252.

27. Andrews, H.L., J.P. Vogel, and R.R. Isberg. 1998. *Legionella pneumophila* genes essential for intracellular growth and evasion of the endocytic pathway. *Infect. Immun.* 66:950–958.

28. Chavrier, P., R.G. Parton, H.P. Hauri, K. Simons, and M. Zerial. 1990. Localization of low molecular weight GTP

binding proteins to exocytic and endocytic compartments. *Cell*. 62:317–329.

29. Berger, K.H., and R.R. Isberg. 1993. Two distinct defects in intracellular growth complemented by a single genetic locus in *Legionella pneumophilia*. *Mol. Microbiology*. 7:7–19.

30. Watarai, M., H.L. Andrews, and R.R. Isberg. 2001. Formation of a fibrous structure on the surface of *Legionella pneumophila* associated with exposure of DotH and DotO proteins after intracellular growth. *Mol. Microbiol*. 39:313–330.

31. Yang, Y., and R.R. Isberg. 1997. Transcriptional regulation of the *Yersinia pseudotuberculosis* pH6 antigen adhesin by two envelope-associated components. *Mol. Microbiol*. 24:499–510.

32. Feeley, J.C., R.J. Gibson, G.W. Gorman, N.C. Langford, J.K. Rasheed, D.C. Makel, and W.B. Blaine. 1979. Charcoal yeast extract agar: primary isolation medium for *Legionella peumophilia*. *J. Clin. Microbiology*. 10:437–441.

33. Gabay, J.E., and M.A. Horowitz. 1985. Isolation and characterization of the cytoplasmic and outer membranes of the *Legionnaire's* disease bacterium (*Legionella pneumophilia*). *J. Exp. Med*. 161:409–422.

34. Kirby, J.E., J.P. Vogel, H.L. Andrews, and R.R. Isberg. 1998. Evidence for pore-forming ability by *Legionella pneumophila*. *Mol. Microbiol*. 27:323–336.

35. McLean, I.W., and P.K. Nakane. 1974. Periodate-lysine-paraformaldehyde fixative: a new fixative for immunoelectron microscopy. *J. Histochem. Cytochem*. 22:1077–1083.

36. Swanson, M.S., and R.R. Isberg. 1996. Identification of *Legionella pneumophilia* mutants that have aberrant intracellular fates. *Infect. Immun*. 64:2585–2594.

37. Mordue, D.G., N. Desai, M. Dustin, and L.D. Sibley. 1999. Invasion by *Toxoplasma gondii* establishes a moving junction that selectively excludes host cell plasma membrane proteins on the basis of their membrane anchoring. *J. Exp. Med*. 190:1783–1792.

38. Growney, J.D., J.M. Scharf, L.M. Kunkel, and W.F. Dietrich. 2000. Evolutionary divergence of the mouse and human *lgn1*/SMA repeat structures. *Genomics*. 64:62–81.

39. Dietrich, W., H. Katz, S.E. Lincoln, H.S. Shin, J. Fredman, N.C. Dracopoli, and E.S. Lander. 1992. A genetic map of the mouse suitable for typing intraspecifc crosses. *Genetics*. 131:423–447.

40. Endrizzi, M., S. Huang, J.M. Scharf, A.-R. Kelter, M. Wirth, L.M. Kunkel, W. Miler, and W.F. Dietrich. 1999. Comparative sequence analysis of the Mouse and Human *Lgn1*/SMA interval. *Genomics*. 60:137–151.

41. Scharf, J.M., D. Damron, A. Frisella, S. Brumo, A.H. Beggs, L.M. Kunkel, and W.F. Dietrich. 1996. The mouse region syntenic for human spinal muscular atrophy lies within the *Lgn1* critical interval and contains multiple copies of *Naip* exon5. *Genomics*. 38:405–417.

42. Swanson, J.A. 1989. Phorbol esters stimulate macropinocytosis and solute flow through macrophages. *J. Cell Sci*. 94:135–142.

43. Clemens, D.L., and M.A. Horwitz. 1992. Membrane sorting during phagocytosis: selective exclusion of major histocompatibility complex molecules but not complement receptor CR3 during conventional and coiling phagocytosis. *J. Exp. Med*. 175:1317–1326.

44. Clemens, D.L., B.Y. Lee, and M.A. Horwitz. 2000. *Mycobacterium tuberculosis* and *Legionella pneumophila* phagosomes exhibit arrested maturation despite acquisition of Rab7. *Infect. Immun*. 68:5154–5166.

45. Abrami, L., M. Fivaz, P.E. Glauser, R.G. Parton, and F.G. van der Goot. 1998. A pore-forming toxin interacts with a GPI-anchored protein and causes vacuolation of the endoplasmic reticulum. *J. Cell Biol*. 140:525–540.

46. Diep, D.B., K.L. Nelson, S.M. Raja, E.N. Pleshak, and J.T. Buckley. 1998. Glycosylphosphatidylinositol anchors of membrane glycoproteins are binding determinants for the channel-forming toxin aerolysin. *J. Biol. Chem*. 273:2355–2360.

47. Yoshida, S., Y. Goto, Y. Mizuguchi, K. Nomoto, and E. Skamene. 1991. Genetic control of natural resistance in mouse macrophages regulating intracellular *Legionella pneumophilia* multiplication in vitro. *Infect. Immun*. 59:428–432.

48. Rittig, M.G., G.R. Burmester, and A. Krause. 1998. Coiling phagocytosis: when the zipper jams, the cup is deformed. *Trends in Microbiology*. 6:384–388.

49. Alpuche-Aranda, C.M., E.P. Berthiaume, B. Mock, J.A. Swanson, and S.I. Miller. 1994. *Salmonella* stimulate macrinocytosis and persist within spacious phagosomes. *J. Exp. Med*. 179:601–608.

50. Alpuche-Aranda, C.M., E.L. Racoosin, J.A. Swanson, and S.I. Miller. 1995. Spacious phagosome formation within mouse macrophages correlates with *Salmonella* serotype pathogenicity and host susceptability. *Infect. Immun*. 63:4456–4462.

51. Racoosin, E.L., and A. Swanson. 1989. Macrophage colony-stimulating factor (M-CSF) stimulates pinocytosis in bone marrow derived macrophages. *J. Exp. Med*. 170:1635–1648.

52. Press, B., Y. Feng, B. Hoflack, and A. Wandinger-Ness. 1998. Mutant Rab7 causes the accumulation of cathepsin D and cation-independent mannose 6-phosphate receptor in an early endocytic compartment. *J. Cell Biol*. 140:1075–1089.

53. Wolf, A.A., M.G. Jobling, S. Wimer-Mackin, M. Ferguson-Maltzman, J.L. Madara, R.K. Holmes, and W.I. Lencer. 1998. Ganglioside structure dictates signal transduction by cholera toxin and association with caveolae-like membrane domains in polarized epithelia. *J. Cell Biol*. 141:917–927.

54. Poussin, C., M. Foti, J.L. Carpentier, and J. Pugin. 1998. CD14-dependent endotoxin internalization via a macropinocytic pathway. *J. Biol. Chem*. 273:20285–20292.

55. Lauer, S., J. VanWye, T. Harrison, H. McManus, B.U. Samuel, N.L. Hiller, N. Mohandas, and K. Haldar. 2000. Vacuolar uptake of host components, and a role for cholesterol and sphingomyelin in malarial infection. *EMBO J*. 19:3556–3564.

56. Kenworthy, A.K., N. Petranova, and M. Edidin. 2000. High-resolution FRET microscopy of cholera toxin B-subunit and GPI-anchored proteins in cell plasma membranes. *Mol. Biol. Cell*. 11:1645–1655.

57. Shin, J.S., Z. Gao, and S.N. Abraham. 2000. Involvement of cellular caveolae in bacterial entry into mast cells. *Science*. 289:785–788.

58. Gatfield, J., and J. Pieters. 2000. Essential role for cholesterol in entry of mycobacteria into macrophages. *Science*. 288:1647–1650.

59. Shin, J.S., and S.N. Abraham. 2001. Review article: co-option of endocytic functions of cellular caveolae by pathogens. *Immunology*. 102:2–7.

60. Diez, E., Z. Yaraghi, A. MacKenzie, and P. Gros. 2000. The neuronal apoptosis inhibitory protein (Naip) is expressed in macrophages and is modulated after phagocytosis and during intracellular infection with *Legionella pneumophilia*. *J. Immunol*. 164:1470–1477.